Journal of Neuroimmunology 236 (2011) 93–98

Contents lists available at ScienceDirect

Journal of Neuroimmunology

journal homepage: www.elsevier.com/locate/jneuroim

Orthogonal array formation by human aquaporin-4: Examination of neuromyelitis optica-associated aquaporin-4 polymorphisms

Jonathan M. Crane [a], Andrea Rossi [a], Tripta Gupta [a], Jeffrey L. Bennett [b], A.S. Verkman [a,*]

[a] Departments of Medicine and Physiology, University of California, San Francisco, CA 94143 USA
[b] Departments of Neurology and Ophthalmology, University of Colorado Denver, Aurora, CO 80045 USA

ARTICLE INFO

Article history:
Received 8 February 2011
Received in revised form 29 April 2011
Accepted 5 May 2011

Keywords:
NMO
AQP4
Water channel
Neuroinflammation

ABSTRACT

Pathogenic autoantibodies target aquaporin-4 (AQP4) water channels in individuals with neuromyelitis optica (NMO). Recently, allelic mutations were reported at residue 19 of AQP4 in three cases of NMO, and it was suggested that polymorphisms may influence disease by altering AQP4 supramolecular assembly into orthogonal arrays of particles (OAPs). We analyzed the determinants of OAP formation by human AQP4 to investigate the possible role of polymorphisms in NMO pathogenesis. NMO-associated mutations R19I and R19T in AQP4 did not affect OAP assembly, palmitoylation-dependent regulation of assembly, or NMO autoantibody binding. Residue-19 polymorphisms in AQP4 are thus unlikely to be disease relevant.

1. Introduction

Aquaporin-4 (AQP4) is a water channel expressed at the plasma membrane in astrocytes in the central nervous system as well as in various peripheral organs such as kidney and skeletal muscle (Frigeri et al., 1995). AQP4 facilitates osmotically driven water transport. Phenotype analysis of AQP4 knockout mice indicated the involvement of AQP4 in brain water balance, neuroexcitation and astrocyte migration (Verkman et al., 2006). AQP4 is the target antigen of autoantibodies in the neuroinflammatory demyelinating disease neuromyelitis optica (NMO), where pathogenic autoantibodies are thought to bind to AQP4, produce astrocyte damage, and initiate a cascade of inflammatory events resulting in myelin loss and neurological impairment (Lennon et al., 2005; Wingerchuk et al., 2007; Jarius et al., 2008).

The AQP4 protein is expressed as two major isoforms: a long isoform, M1, with translational initiation at Met-1, and a shorter isoform, M23, with translational initiation at Met-23 (Yang et al., 1995; Lu et al., 1996). AQP4 can form supramolecular assemblies in membranes called orthogonal arrays of particles (OAPs), which are square arrays of particles visualized by freeze-fracture electron microscopy (Wolburg, 1995). M23 by itself forms large OAPs in transfected cells (Yang et al., 1996), whereas M1 by itself forms few or no OAPs. However, M1 can co-associate with M23 to form mixed-composition OAPs that are smaller than the OAPs formed by M23 alone (Furman et al., 2003). Using multiple independent techniques, we found that M1 and M23 can assemble as heterotetramers, and that OAPs are dynamic structures that are subject to regulation by second messengers and N-terminus palmitoylation at residues Cys-13 and Cys-17 (Crane et al., 2009; Tajima et al., 2010). Truncation and mutagenesis indicated that OAP formation by M23 involves N-terminus M23–M23 inter-tetrameric interactions, and that the inability of M1 to form OAPs involves blocking of the N-terminus interaction by residues just upstream of Met-23 (Crane and Verkman, 2009).

The causative factors in the generation of pathogenic AQP4 autoantibodies in NMO are not known. A genetic susceptibility has been proposed based on increased disease occurrence in related than unrelated persons (Matiello et al., 2010). The possible involvement of AQP4 polymorphisms in NMO was proposed from the observation that 3 out of 172 NMO patients had mutations at Arg-19 (R19I and R19T), whereas control subjects did not (Matiello et al., 2009a, b). Based on data that some AQP4 autoantibodies bind more tightly to OAPs than to individual AQP4 tetramers (Nicchia et al., 2009; Mader et al., 2010; Crane et al., 2011), and on the involvement of the AQP4 N-terminus in OAP formation/disruption (Crane et al., 2009), it was speculated that the residue-19 polymorphisms may alter OAP formation by AQP4 and hence autoantibody binding (Matiello et al., 2009a, b). Here, we tested this possibility by a series of biophysical and biochemical measurements on native human AQP4 and human Arg-19 AQP4 mutants.

2. Materials and methods

2.1. DNA constructs, cell culture and transfections

DNA constructs encoding human AQP4 isoforms were generated by PCR-amplification using whole brain cDNA as template. Myc-

* Corresponding author at: 1246 Health Sciences East Tower, University of California, San Francisco, San Francisco, CA 94143–0521, USA. Tel.: +1 415 476 8530; fax: +1 415 665 3847.
E-mail address: alan.verkman@ucsf.edu (A.S. Verkman).
URL: http://www.ucsf.edu/verklab (A.S. Verkman).

0165-5728/$ – see front matter © 2011 Elsevier B.V. All rights reserved.
doi:10.1016/j.jneuroim.2011.05.001

tagged AQP4 was generated as previously described. AQP4 mutants were generated by PCR-amplification using either tagged or non-tagged templates. PCR fragments were ligated into mammalian expression vector pcDNA3.1 and fully sequenced. COS-7 (ATCC CRL-1651) and U87MG (ATCC HTB-14) cell cultures were maintained at 37 °C in 5% CO_2/95% air in the appropriate medium containing 10% fetal bovine serum, 100 U/mL penicillin and 100 μg/mL streptomycin.

2.2. Single particle tracking

COS-7 cells were grown on 18-mm diameter glass coverslips and transfected in Lipofectamine 2000 (Invitrogen, Carlsbad, CA) with DNA encoding Myc-tagged AQP4 isoforms and mutants. 12–24 h after transfection, cells were washed with 2 mL PBS containing 6 mM glucose and 1 mM pyruvate (GP buffer) and incubated for 5 min in blocking buffer. Cells were then incubated for 5 min with 70 ng/mL mouse anti-Myc antibody (Covance, Emeryville, CA) in blocking buffer, rinsed, and incubated for 5 min with 0.1 nM goat $F(ab')_2$ anti-mouse IgG-conjugated Qdot 655 (Invitrogen) in blocking buffer. Cells were rinsed extensively and maintained throughout experiments in GP buffer. SPT was performed on a Nikon Eclipse TE2000S inverted epi-fluorescence microscope (Nikon, Melville, NY) equipped with a Nikon 100x TIRF oil immersion objective (numerical aperture 1.45) and a deep-cooled CCD camera (Hamamatsu EM-CCD, Bridgewater, NJ). Qdot fluorescence was excited using an E460SPUV excitation filter and 475DCXRU dichroic mirror, and detected through a D655/40 m emission filter (Chroma, Rockingham, VT). Data were acquired continuously at 11 ms per frame (91 Hz) for 6 s. Image sequences were analyzed and trajectories constructed as described previously (Crane et al., 2008). Diffusion data are reported as averaged diffusion coefficients and cumulative distributions of range at 1 s, where P (range) is defined as the probability that a particle's range is less than or equal to a given distance at $t = 1$ s.

2.3. Electrophoresis and immunoblotting

48 h prior to lysis, U87MG cells were transfected using Lipofectamine 2000 with DNA encoding AQP4 isoforms and mutants. Cultures were lysed with NativePAGE sample buffer (Invitrogen) containing 1% dodecyl-β-D-maltoside (EMD chemicals, Gibbstown, NJ) for 10 min on ice. Lysates were centrifuged at 20,000 *g* for 30 min at 4 °C and the pellet discarded. Blue-native gel electrophoresis (BN-PAGE) was performed with polyacrylamide native gradient gels (3–9%). 10 μg of protein was mixed with 5% Coomassie Blue G-250 (Invitrogen) and loaded in each lane. Ferritin was used as the molecular mass standard (440 and 880 kDa). Running buffers were: 25 mM imidazole, pH 7 (anode buffer) and 50 mM Tricine, 7.5 mM imidazole, 0.02% Coomassie Blue G-250, pH 7 (cathode buffer). Tricine SDS-PAGE was performed with a 12% running gel and 3% stacking gel. SeeBlue Plus2 Pre-Stained Standard (Invitrogen) was used as a molecular weight marker. Proteins were blotted onto polyvinyl difluoride membranes (Bio-Rad, Hercules, CA). For immunoblot analysis, membranes were blocked with 3% BSA and incubated with rabbit anti-AQP4 primary antibodies (Santa Cruz Biotechnology, Santa Cruz, CA), then rinsed and incubated with horseradish peroxidase-conjugated goat anti-rabbit IgG (Jackson ImmunoResearch), rinsed extensively, and labeled proteins were detected using the ECL Plus enzymatic chemiluminescence kit (Amersham Biosciences, Pittsburgh, PA).

2.4. Quantitative immunofluorescence

NMO serum was obtained from four seropositive individuals who met the revised diagnostic criteria for clinical disease (Wingerchuk et al., 2006). U87MG cells were grown on 12 mm glass coverslips and transfected in Lipofectamine 2000 with DNA encoding AQP4 isoforms and mutants. 12–24 h after transfection, cells were incubated for 20 min in live-cell blocking buffer (PBS containing 6 mM glucose, 1 mM pyruvate, 1% bovine serum albumin, 2% goat serum), and then for

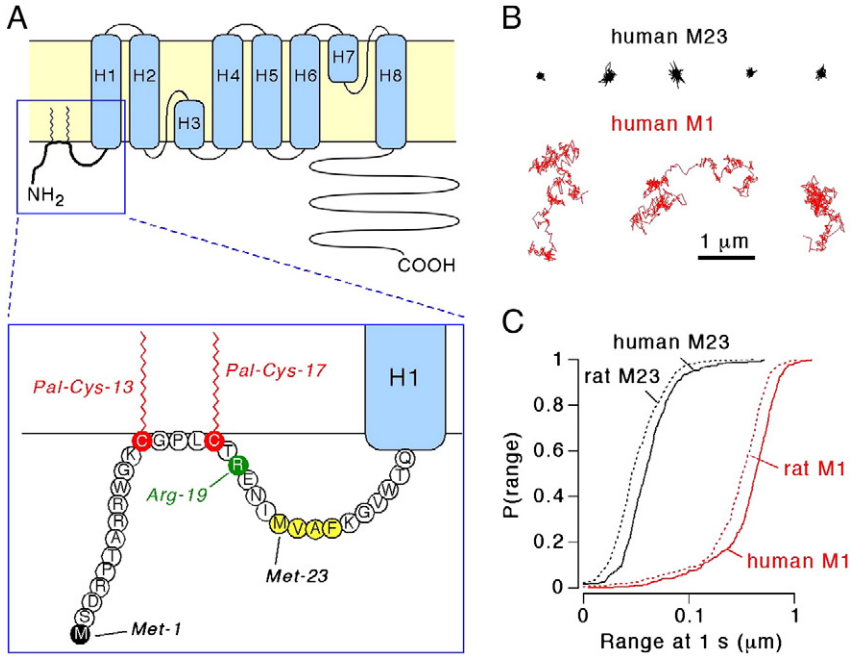

Fig. 1. OAP-forming properties of human AQP4. A. Schematic diagram of the N-terminus of M1 AQP4 showing the human sequence. Sites of cysteine palmitoylation are shown in red. Arg-19, which is mutated in a small subset of NMO patients, is shown in green. Hydrophobic residues that are required for OAP assembly by M23 AQP4 are shown in yellow. Transmembrane domains are shown in light blue. B. Representative single particle trajectories from quantum dot-labeled human AQP4 isoforms M23 (black) and M1 (red). Trajectories were acquired at 91 Hz for 6 s. Bar, 1 μm. C. Cumulative distribution of the diffusion range at 1 s for AQP4 isoforms M23 (black) and M1 (red). Both human (solid) and rat (dotted) diffusion profiles are shown for comparison.